



ALMA MATER STUDIORUM
UNIVERSITÀ DI BOLOGNA

ARCHIVIO ISTITUZIONALE DELLA RICERCA

Alma Mater Studiorum Università di Bologna Archivio istituzionale della ricerca

Smartphone biosensor for point-of-need chemiluminescence detection of ochratoxin A in wine and coffee

This is the final peer-reviewed author's accepted manuscript (postprint) of the following publication:

Published Version:

Zangheri, M., Di Nardo, F., Calabria, D., Marchegiani, E., Anfossi, L., Guardigli, M., et al. (2021). Smartphone biosensor for point-of-need chemiluminescence detection of ochratoxin A in wine and coffee. *ANALYTICA CHIMICA ACTA*, 1163, 1-10 [10.1016/j.aca.2021.338515].

Availability:

This version is available at: <https://hdl.handle.net/11585/863418> since: 2022-02-22

Published:

DOI: <http://doi.org/10.1016/j.aca.2021.338515>

Terms of use:

Some rights reserved. The terms and conditions for the reuse of this version of the manuscript are specified in the publishing policy. For all terms of use and more information see the publisher's website.

This item was downloaded from IRIS Università di Bologna (<https://cris.unibo.it/>).
When citing, please refer to the published version.

(Article begins on next page)

This is the final peer-reviewed accepted manuscript of:

Martina Zangheri, Fabio Di Nardo, Donato Calabria, Elisa Marchegiani, Laura Anfossi, Massimo Guardigli, Mara Mirasoli, Claudio Baggiani, Aldo Roda. Smartphone biosensor for point-of-need chemiluminescence detection of ochratoxin A in wine and coffee. *Analytica Chimica Acta*, Volume 1163, 2021, 338515

The final published version is available online at:

<https://www.sciencedirect.com/science/article/pii/S000326702100341X>

Terms of use:

Some rights reserved. The terms and conditions for the reuse of this version of the manuscript are specified in the publishing policy. For all terms of use and more information see the publisher's website.

This item was downloaded from IRIS Università di Bologna (<https://cris.unibo.it/>)

When citing, please refer to the published version.

Smartphone biosensor for point-of-need chemiluminescence detection of ochratoxin A in wine and coffee

Martina Zangheri^{a,b}, Fabio Di Nardo^c, Donato Calabria^a, Elisa Marchegiani^a, Laura Anfossi^c, Massimo Guardigli^{a,e}, Mara Mirasoli^{a,d,e}, Claudio Baggiani^c, Aldo Roda^{a,d}

^a Department of Chemistry "Giacomo Ciamician", Alma Mater Studiorum - University of Bologna, Via Selmi 2, 40126, Bologna, Italy

^b Interdepartmental Centre of Industrial Agrifood Research (CIRI Agrifood), Alma Mater Studiorum, University of Bologna, Piazza Goidanich 60, 47521, Cesena, Italy

^c Department of Chemistry, University of Turin, Via P. Giuria 5, 10125, Torino, Italy

^d Interuniversity Consortium "Istituto Nazionale Biostrutture e Biosistemi" (INBB) - Viale Delle Medaglie D'Oro 305, 00136, Roma, Italy

^e Interdepartmental Centre of Industrial Research "Renewable Sources, Environment, Blue Growth, Energy", University of Bologna, Via Angherà 22, Rimini, 47921, Italy

This item was downloaded from IRIS Università di Bologna (<https://cris.unibo.it/>)

When citing, please refer to the published version.

Abstract

Exposure to mycotoxins, which may contaminate food and feed commodities, represents a serious health risk for consumers. Ochratoxin A (OTA) is one of the most abundant and toxic mycotoxins, thus specific regulations for fixing its maximum admissible levels in foodstuff have been established. Lateral Flow ImmunoAssay (LFIA)-based devices have been proposed as screening tools to avoid OTA contamination along the whole food chain. We report a portable, user-friendly smartphone-based biosensor for the detection and quantification of OTA in wine and instant coffee, which combines the LFIA approach with chemiluminescence (CL) detection. The device employs the smartphone camera as a light detector and uses low-cost, disposable analytical cartridges containing the LFIA strip and all the necessary reagents. The analysis can be carried out at the point of need by non-specialized operators through simple manual operations. The biosensor allows OTA quantitative detection in wine and coffee samples up to $25 \mu\text{g L}^{-1}$ and with limits of detection of 0.3 and $0.1 \mu\text{g L}^{-1}$, respectively, which are below the European law-fixed limits. These results demonstrate that the developed device can be used for routine monitoring of OTA contamination, enabling rapid and reliable identification of positive samples requiring confirmatory analysis.

Keywords

Lateral flow immunoassay, Ochratoxin A, Chemiluminescence, Smartphone, Food safety, Mycotoxins, Point of need.

This item was downloaded from IRIS Università di Bologna (<https://cris.unibo.it/>)

When citing, please refer to the published version.

1. Introduction

Food safety is a global health priority and a key factor to safeguarding the well-being of people, pursuing food security, and fostering economic development. The World Health Organization (WHO) has estimated that 600 million cases of foodborne illnesses and 420,000 related deaths occur annually [1]. Among strategies to overcome foodborne diseases, WHO has emphasized the importance of providing consumers with tools to make safe food choices. In addition, food contamination has a relevant economic impact in terms of both market loss and public health impact. For example, it has been estimated that the Serbian farm-level dairy sector suffered a loss of more than 90 million euros from the aflatoxins outbreak in 2013 [2]. Thus, the availability of reliable, sensitive, and fast portable analytical devices will also contribute to reduce social and financial burden of food contamination.

Smartphone-based biosensors based on optical detection principles have recently emerged as powerful tools with the potential to revolutionize food testing by engaging farmers or consumers in their own food safety analysis. Indeed, smartphones represent an ideal facilitator for point-of-need devices, as they combine pervasive distribution with rapidly developing technologies for connectivity, customizable applications, image acquisition and processing into multifunctional, pocket-sized devices [[3], [4], [5], [6], [7]]. Integration with paper-based assay technology provides simple, cheap, and portable analytical devices that meet the needs of commercial applications in outbreak control, food chain monitoring and regulatory inspection [[5], [6], [7], [8], [9]]. In this context, consumer-friendly smartphone-based biosensors have been already developed for detecting food allergens [7,10], pathogens [[11], [12], [13], [14], [15], [16]] and chemical contaminants [[17], [18], [19], [20], [21], [22]]. Mycotoxins are fungal secondary metabolites highly toxic to humans and cattle. The Food and Agriculture Organization (FAO) of the United Nations has estimated that mycotoxins contaminate 25% of the world's food crops [23]. Filamentous fungi proliferate in food commodities in environmental conditions (i.e., temperature, humidity, and sunlight) typical of tropical and subtropical countries. Food production globalization (involving long storage and transportation times) and climate changes (causing temperature rise in cool or temperate countries) further increases the risk of mycotoxins widespread contamination [6,24,25]. This points out the need for portable analytical devices for rapid mycotoxin detection along the whole food supply chain and at the consumer endpoint [26,27]. Indeed, following the Citizen Science approach, appropriate smartphone-based biosensors would provide personalized food testing, also enabling controls intensification by involving consumers in testing activities and exploiting shared databases and geolocalized warning systems [28]. In addition, the availability for self-testing technologies could have a substantial positive effect in developing countries, where significant dangerous contaminations can still occur and access to centralized laboratories is not possible. In these settings, smartphone-based analytical platforms could be used for testing along the local food chain [6]. However, the potential of smartphone-based optical biosensors for mycotoxins monitoring is still underexplored and only few examples have been reported in the literature [14,[29], [30], [31]].

In this context, we propose a portable and user-friendly smartphone-based biosensor for the detection of Ochratoxin A (OTA), a mycotoxin with cytotoxic, carcinogenic, mutagenic, and immunosuppressive activity, in wine and instant coffee [32,33]. Wine and coffee represent

This item was downloaded from IRIS Università di Bologna (<https://cris.unibo.it/>)

When citing, please refer to the published version.

important sources of OTA dietary intake for the EU population, posing a serious risk for human health. Hence, maximum admissible levels as low as $2 \mu\text{g kg}^{-1}$ and $10 \mu\text{g kg}^{-1}$ have been established by the European Union in wine and instant coffee, respectively (the limit decreases to $5 \mu\text{g kg}^{-1}$ for roasted coffee beans and ground roasted coffee) [34]. The same values have also been set by Canada [35], but specific legislation on this topic is missing in most extra-European countries.

The proposed biosensor is based on Lateral Flow Immunoassay technique coupled with chemiluminescence detection (CL-LFIA). CL provides enhanced analytical performance with respect to visual detection (e.g., exploiting gold nanoparticles as labels), often employed for readout of LFIA assays. In addition, CL is an ideal detection principle since it combines simplicity of signal measurement, amenability to miniaturization, and wide dynamic range [[36], [37], [38], [39], [40], [41]]. The latter could be particularly advantageous for developing a method characterized by a dynamic range suitable for application for analysis of both wine and instant coffee, despite the different regulatory limits. The biosensor consists in a smartphone-integrated self-standing device comprising a low-cost and disposable analytical cartridge containing all the reagents required for the execution of the analysis. The cartridge can be used through simple manual operations and the entire analysis can therefore be carried out at the point of need by non-specialized operators using the smartphone CMOS (Complementary Metal-Oxide Semiconductor) camera as light detector. Analysis relies on a competitive immunoassay, in which OTA in the sample and a horseradish peroxidase OTA conjugate (HRP-OTA) compete for a limited amount of an anti-OTA antibody immobilized on the LFIA nitrocellulose strip. The HRP-OTA bound to immobilized antibody is then detected by CL upon addition of an HRP CL substrate based on luminol/ H_2O_2 and enhancers. According to the competitive format, the amount of HRP-OTA bound, and thus the intensity of the CL signal, are inversely related to the amount of OTA in the sample. The proposed system allows the reliable quantification of OTA as required by the current regulations and could thus be used as a first-level screening analytical tool for detecting potentially contaminated samples to be subjected to confirmatory analysis with reference instrumental analytical methods.

2. Materials and methods

2.1. Reagents

The polyclonal anti-OTA antibody produced in rabbit and the HRP-OTA conjugate were kindly provided by Euroclone SpA (Milan, Italy). Polyclonal anti-HRP antibody produced in rabbit, ovalbumin (OVA), Tween-20, polyethylene glycol 10000, and mycotoxin standards (Aflatoxin B1, Aflatoxin B2, Aflatoxin G1, Aflatoxin G2, Fumonisin B1, Fumonisin B2, and Zearalenone Oekanal certified solutions), were obtained from Sigma-Aldrich Co (St. Louis, MO). The CL HRP detection substrate Supersignal ELISA Femto was purchased from Thermo Scientific Inc. (Rockford, IL). The other reagents were of analytical grade and were employed as received. Phosphate buffered saline (PBS), pH 7.4, contained $10 \text{ mmol L}^{-1} \text{Na}_2\text{HPO}_4$, $2 \text{ mmol L}^{-1} \text{KH}_2\text{PO}_4$, $137 \text{ mmol L}^{-1} \text{NaCl}$, $2.7 \text{ mmol L}^{-1} \text{KCl}$. The LFIA strips were produced using Whatman Standard 14 glass fibre sample pad (GE Healthcare Lifescience, Chalfont St. Giles, UK), Hi-flow plus 180 nitrocellulose membrane cards (Merck Millipore, Billerica, MA), and cellulose absorbent pads (Merck Millipore).

2.2. Preparation of the LFIA strips

This item was downloaded from IRIS Università di Bologna (<https://cris.unibo.it/>)

When citing, please refer to the published version.

Anti-OTA antibody 1:50 (v/v) and anti-HRP antibody 1:500 (v/v) solutions in 20 mM phosphate buffer (PB) at pH 7.4 were applied onto the nitrocellulose (NC) membrane cards to form the Test line (T-line) and the Control line (C-line), respectively, by a XYZ3050 dispenser platform (Biodot, Irvine, CA). The solutions were non-contact dispensed at $1 \mu\text{L cm}^{-1}$ keeping a distance of 5 mm between the two lines. The NC cards were dried at 37°C for 45 min under vacuum, saturated with 1% (w/v) OVA in PB, washed with PB supplemented with 0.05% (v/v) Tween-20, and finally dried under vacuum at 37°C for 90 min. The sample pads were saturated with PB supplemented with 3% (w/v) OVA and 0.1% (v/v) Tween-20, then dried for 90 min at 40°C . The cards were laminated with the sample and absorbent pads, then cut by a CM400 guillotine (Biodot) to obtain 5-mm width LFIA strips. The strips were sealed in plastic bags containing a silica desiccant and stored at room temperature in the dark until use.

2.3. Analytical device

The analytical device includes two components, a disposable analytical cartridge, and a mini dark box with a smartphone holder. The latter hosts the cartridge during the measurement of the CL signal.

The disposable analytical cartridge (Fig. 1) consists of a plastic holder (size $110 \times 90 \times 4$ mm) containing a fluidic element that houses the LFIA strip, the reagents necessary for the analysis and the fluidic system for metering the correct amount of sample and for transferring sample and reagents to the LFIA strip.

The fluidic element is composed of two 200- μm transparent polypropylene layers. The upper layer has embossed chambers, valves and channels obtained by vacuum thermoforming while the bottom one is flat and adhesive to allow assembly of the fluidic element. The upper layer contains, in addition to the fluidic channels, the following components: (a) a 30- μL sample metering chamber; (b) a sample overflow chamber; (c) three reservoirs for the pouches containing the OTA-HRP conjugate solution and the two components (luminol/enhancer and oxidant) of the SuperSignal ELISA Femto HRP CL substrate; (d) two manually actuated valves for controlling sample and reagents flow; (e) a cavity for the LFIA strip, also hosting a large additional adsorbent pad to further promote flow of sample and reagents along the LFIA strip. For sample loading, a unidirectional valve is connected to the fluidic element by a short PEEK tube. Positions of the components of the fluidic element and their connections are shown in detail in Fig. 1A.

The plastic holder protects the fluidic element and supports the unidirectional valve for sample loading, thus acting as an interface towards the sampling equipment.

The analytical cartridge was prepared in advance prior to the analysis. OTA-HRP conjugate solution was prepared by dilution 1:2500 (v/v) in PBS supplemented with 3% (w/v) OVA as a saturating agent to reduce nonspecific binding. Then, three vacuum thermoformed polypropylene reagent pouches were filled with the reagents (60 μL of OTA-HRP conjugate and 40 μL each of the two components of the CL HRP detection substrate) and sealed with adhesive tape. Subsequently, the fluidic element was assembled after inserting the reagent pouches, the LFIA strip and the additional absorbent pad, connected to the sample loading valve and glued between the two halves of the plastic holder.

This item was downloaded from IRIS Università di Bologna (<https://cris.unibo.it/>)

When citing, please refer to the published version.

For performing CL measurement, the analytical cartridge was inserted in a mini dark box to avoid ambient light interference (Fig. 2). The mini dark box is equipped with an adapter for the OnePlus 6 smartphone (OnePlus, Shenzhen, China) and a plano-convex lens (diameter 6 mm, focal length 9 mm, Edmund Optics, York, UK) to enable correct imaging of the LFIA strip by the smartphone camera.

The fluidic element plastic holder and the mini dark box have been designed using the browser-based 3D design platform Tinkercad (Autodesk, San Rafael, CA) and produced in black acrylonitrile-butadiene-styrene (ABS) copolymer using a Makerbot Replicator 2X printer (Makerbot Industries, New York, NY) exploiting Fused Deposition Modelling (FDM) 3D printing technology.

2.4. Assay procedure

The analysis procedure is shown in Fig. 3. While keeping the flow control valves in the “sample inject” position, the sample was injected using a syringe connected to the sample loading valve, until the sample metering chamber was filled, and excess sample arrived at the sample overflow chamber (Fig. 3B). Then, upon shifting the flow control valves to the “analysis” position, the HRP-OTA chamber was pushed, thus squeezing the inner reagent pouch. This transferred both the sample and the HRP-OTA conjugate solution to the sample pad of the LFIA strip, (Fig. 3C). The mixed solutions began flowing across the membrane where the immunoreactions took place. Upon complete migration across the LFIA strip (30 min), the HRP CL substrate was added to the strip by simultaneously pushing the other two chambers (Fig. 3D). After 15 min the analytical cartridge was inserted into the mini dark box connected to the smartphone and the CL signal was measured using a 4-sec exposure time. For the correct assay performance, the analysis should be performed at room temperature (e.g., between 15 and 30 °C). Since the analytical cartridges are stored at +4 °C, they must be brought to room temperature prior to the assay.

To obtain quantitative information on the OTA content of samples, CL images were analyzed by the freely available image analysis software ImageJ (v. 1.53c, National Institutes of Health, Bethesda, MD). For each sample, the photon emissions corresponding to the C-line and the T-line of the LFIA strip were calculated by integrating the CL signal in the line areas and subtracting the background signal obtained by averaging the CL signals measured in two areas just below and above each line. Then, the T-line/C-line CL signal ratio was calculated, and the concentration of OTA was determined by interpolation on calibration curves generated by analysing matrix-matched standard OTA solutions (concentration range 0–25 $\mu\text{g L}^{-1}$) in wine or coffee matrices, plotting the corresponding T-line/C-line CL signal ratios against the analyte concentration in logarithmic scale and fitting the resulting sigmoidal curve with a four-parameter logistic equation. Data graphing and fitting were performed using the Prism data graphing and analysis software (v. 8.0.3, GraphPad Software, San Diego, CA).

2.5. Analysis of real samples

Red or white wine and instant coffee samples were obtained directly from local stores. Instant coffee was dissolved in hot water (80 °C) at a concentration of 50 g solid L^{-1} , then let cool to room temperature. To remove substances that could interfere with the CL detection (e.g., polyphenols) samples were subjected to a pre-analytical procedure developed for wine matrices by Anfossi et al.

This item was downloaded from IRIS Università di Bologna (<https://cris.unibo.it/>)

When citing, please refer to the published version.

[42], with slight modifications. Briefly, sample solutions were thoroughly mixed with 0,15 M NaHCO₃ (pH 9.0) and 4% (w/v) PEG 10000 water solutions in the 1:2:2 (v/v) ratio and let react for a few minutes before analysis. Matrix-matched standard OTA solutions used for the generation of calibration curves were prepared in wine or coffee blank matrices subjected to the same pre-analytical treatment.

For evaluation of assay performance, the OTA content of the samples was also determined by a previously described HPLC-FLD reference method [43]. The chromatographic separation was carried out on a C₁₈ RP column operating in an isocratic mode with an acetonitrile–water–acetic acid 55:44:1 (v/v/v) mobile phase at a flow rate of 1.0 mL min⁻¹. The target analyte was detected using a fluorescence detector ($\lambda_{\text{ex}} = 333 \text{ nm}$, $\lambda_{\text{em}} = 460 \text{ nm}$) and its concentration was determined by interpolating peak areas on a calibration curve generated by analyzing standard OTA solutions, plotting the peak areas against OTA concentration, and fitting the data using a weighted linear regression model (weight = 1/x). The HPLC-FLD reference method has a limit of quantification (LOQ) of 0.1 $\mu\text{g L}^{-1}$ OTA and a mean relative standard deviation (RSD) of 21% in the concentration working range (0,1–10 $\mu\text{g L}^{-1}$).

3. Results and discussion

The LFIA-CL device couples an analytical element (the disposable analytical cartridge) with a smartphone for CL signal readout and provides high flexibility in terms of smartphone interface. This is a crucial point for pursuing wide applicability of a smartphone-based biosensor since each brand commercializes several new smartphone models every year. The mini dark box can be used with different smartphones by simply designing smartphone adapters fitted with the given mobile device. Adapters can be then produced rapidly and at low cost thanks to the versatility of the 3D printing technology. In terms of camera sensitivity, the performance of actual smartphones is so high that all medium- or high-end products available on the market are suitable for the acquisition of the CL signal. It should be also pointed out that our approach, rather than transforming the smartphone into a lab device, exploits the built-in smartphone technology in a non-invasive way, still retaining the smartphone's full functionality and integrity [44].

This smartphone-based CL-LFIA device represents an advancement over the previously published one [37], since it has been optimized for point-of-use application. In particular, the analytical cartridge has been designed and tested for long term storage and to simplify the operator task thanks to its internal sample metering system, which controls the amount of sample delivered to the LFIA strip eliminating the need for precise sample loading. We also took advantage of our previous experience on fluidic cartridges [45,46] to improve the operation of flow control valves and to reduce the overall size, weight, and cost of the cartridge. As the analytical cartridges are disposable and need refrigeration, this is an advantage from both an economic and logistical point of view (i.e., less space required for shipping and storage of cartridges at controlled temperature).

3.1. Design of the fluidic cartridge

The fluidic cartridge contains all the reagents in a portable and easy to use format, still ensuring the correct and reproducible handling of samples and reagents.

This item was downloaded from IRIS Università di Bologna (<https://cris.unibo.it/>)

When citing, please refer to the published version.

All elements of the fluidics (i.e., the reagents chambers and the sample metering chamber) were dimensioned considering the channels' dead volume, to deliver the desired volumes of sample and reagents to the LFIA strip.

During the analytical protocol, the flows of sample and reagents are driven by applying finger pressure on the reagent chambers and then by capillary force along the LFIA strip. Two valves, each of them constituted by a cavity containing a rectangular-shaped PDMS mobile element, were developed to control the direction of flow. The inner PDMS element of the valve is manually shifted between the two sides of the cavity to open/close the desired flow channels. In more detail, the first valve (located after the sample injection unidirectional valve) had the task of controlling the inlet (sample or OTA-HRP conjugate) of the sample metering chamber. The second valve, located just after the sample metering chamber, controls the outlet of the chamber by driving the fluid to the sample overflow chamber or to the LFIA strip. During the analysis, the mobile elements of the valves were shifted from the left side ("sample inject" position) to the right side ("analysis" position) of the cavities.

An important issue in the analytical procedure, which could affect assay performance, is correct reagents mixing. In particular, while it was expected that the two components of the CL substrate were completely mixed in the serpentine channel before arriving to the LFIA strip, the mixing of the sample and the HRP-OTA conjugate before delivering to the LFIA strip was investigated. Indeed, according to the design of the analytical cartridge, the flow of the HRP-OTA conjugate pushed the sample from the sample metering chamber to the LFIA strip. Therefore, since mixing of the two solutions inside the sample metering chamber is expected to be inefficient, at least part of the sample arrived to the LFIA strip before the HRP-OTA conjugate. We investigated this phenomenon by analysing OTA standard solutions prepared in an OTA-free wine matrix, using two slightly different protocols. In the first one (which represented the ideal analytical procedure) a solution containing both OTA and HRP-OTA conjugate was dispensed on the sample pad of the LFIA strip. In the second protocol (which simulated the real analytical procedure) the OTA and HRP-OTA conjugate solutions were sequentially dispensed on the sample pad. In comparison to the ideal analytical procedure, the sequential addition protocol produced higher decreases of the T-line/C-line CL signal ratios. This behaviour could be ascribed to the fact that in the sequential addition protocol the first aliquot of solution flowing along the LFIA strip was enriched in sample, so that OTA in the sample was favoured in the competition for binding the immunoreagents immobilized in the T-line (the CL signal of the C-line is not affected because the binding of the excess HRP-OTA conjugate is not a competitive process). Nevertheless, the differences in the T-line/C-line CL signal ratio were small, thus it was concluded that the sequential addition of the sample and the HRP-OTA did not negatively affect assay performance.

We also observed a relatively slow flow along the LFIA strip in the cartridge, which was attributed to the absence of evaporation that could accelerate the process. Since complete migration of sample and HRP-OTA conjugate solutions toward the adsorbent should take place before delivering the CL substrate to the LFIA strip, the analytical protocol provided a 30-min interval between the delivering of sample and HRP-OTA solutions and of CL substrate to the LFIA strip. An appropriate time interval (i.e., 15 min) was also provided between delivering of the CL substrate to the LFIA strip

This item was downloaded from IRIS Università di Bologna (<https://cris.unibo.it/>)

When citing, please refer to the published version.

and CL measurement, since the CL substrate had the dual function of developing the CL signal and washing the membrane from unbound species (thus reducing the CL background signal).

3.2. Optimization of experimental parameters

Assay parameters were optimized to achieve limits of detection (LODs) and dynamic ranges useful for detecting OTA in wine and instant coffee according to the current regulatory limits (i.e., $2 \mu\text{g kg}^{-1}$ and $10 \mu\text{g kg}^{-1}$ for wine and instant coffee, respectively). As target OTA concentrations corresponding to the regulatory limits, we considered $2 \mu\text{g L}^{-1}$ for wine (assuming a density of 1 kg L^{-1}) and $0.5 \mu\text{g L}^{-1}$ for instant coffee (taking into account the overall solid concentration in the instant coffee solution). Different HRP-OTA conjugate dilutions, namely 1:1000, 1:2500 and 1:5000 (v/v), were evaluated by comparing the CL signals obtained by analysing OTA-free wine and instant coffee samples before and after spiking with known amounts of OTA; different LFIA strips in which the anti-OTA antibody was immobilized on the T-line either at 1:50 or at 1:100 (v/v) dilutions were employed. As a capture anti-OTA antibody, we selected a polyclonal antibody to maximize the target analyte capture ability. Polyclonal antibodies often have higher affinities than monoclonal ones and, upon immobilization on nitrocellulose, they are less prone to a reduction of binding ability due to conformational changes. These aspects are important in LFIAs since the sample flows across the lines on the nitrocellulose strip, thus binding events must occur in a very limited time and in a restricted spatial area [47]. Despite this advantage, it must be considered that supplies of polyclonal antibodies are subject to variability, thus use of a different polyclonal antibody pool may require assay re-optimization. Based on results shown in Fig. 4, the 1:2500 (v/v) HRP-OTA conjugate dilution and the 1:50 (v/v) anti-OTA antibody dilution immobilized on the T-line were selected as the most suitable for the OTA detection at regulatory limits. Indeed, they provided the most intense CL signals, thus facilitating CL measurement with the smartphone camera, and they allowed clear discrimination from blanks and samples at higher OTA concentration of wine and instant coffee samples containing $2 \mu\text{g L}^{-1}$ and $0.5 \mu\text{g L}^{-1}$ OTA, respectively.

3.3. Calibration curves

Matrix-matched calibration curves were obtained in the optimized experimental conditions by analysing OTA-free wine and instant coffee samples spiked with known amounts of OTA, up to $25 \mu\text{g L}^{-1}$. Being the assay a competitive one, the CL intensity of the T-line was inversely proportional to the concentration of the analyte in the sample and the T-line disappeared for the highest OTA concentrations (Fig. 5A). In this context, it should be mentioned that the calibration curve was generated considering the T-line/C-line CL signal ratio as the analytical signal instead of the CL signal of the T-line alone. This normalization improved assay accuracy by ruling out factors, such as ambient temperature or presence of HRP inhibitors in the sample. Indeed, both the T-line and C-line CL signals derive from the same chemical reaction, therefore their ratio only depends on OTA concentration and not on factors affecting the rate of HRP-catalysed CL reaction (see Fig. 5B).

As shown in Fig. 5C, the calibration curves obtained in the two matrices are very similar to each other, suggesting that the pre-treatment procedure efficiently removed any sample component that might interfere with the assay. The LODs of the assay, calculated as the OTA concentration giving a T-line/C-line CL signal ratio corresponding to that of the blank minus three times its standard

This item was downloaded from IRIS Università di Bologna (<https://cris.unibo.it/>)

When citing, please refer to the published version.

deviation, were $0.3 \mu\text{g L}^{-1}$ and $0.1 \mu\text{g L}^{-1}$ in wine and instant coffee matrices, respectively, while dynamic ranges extended up to the maximum OTA concentration ($25 \mu\text{g L}^{-1}$). The LOD values obtained are comparable to those reported in the literature for other OTA LFIA-based assays, as well as to those of commercial LFIA assay kits (Table 1). The assay also showed a good reproducibility, with RSD associated to the points of the calibration curve always below 12% (wine matrix) and 7% (instant coffee matrix).

3.4. Cartridge stability

While antibodies immobilized on nitrocellulose strips and commercial HRP CL substrates are known to be stable at $+4 \text{ }^\circ\text{C}$ for long periods, the HRP-OTA conjugate is more sensitive to storage conditions. Therefore, we evaluated the long-term stability of disposable analytical cartridges at the storage temperature of $4 \text{ }^\circ\text{C}$ by an accelerated stability test. Briefly, several disposable cartridges were stored at $37 \text{ }^\circ\text{C}$ for up to 4 weeks. In such conditions, each week of conservation roughly corresponds to 1 year of storage at $4 \text{ }^\circ\text{C}$ [55]. Cartridge performance was assessed upon different storage times by analysing an OTA-free wine sample and comparing the results with those obtained using a freshly prepared analytical cartridge. According to the results of the test, the shelf life of the analytical cartridges at $4 \text{ }^\circ\text{C}$ was estimated to be about one year.

3.5. Sample pretreatment

Wine and coffee contain, among others, antioxidant substances that can interfere with the HRP-catalysed luminol oxidation reaction, by deactivating the intermediate radical species that lead to the photon emission. It is therefore necessary to remove these substances prior to analysis. Since the proposed biosensor was designed to be employed directly on site, the sample pretreatment must also be as simple as possible. In this view, the wine sample pre-treatment procedure described by Anfossi et al. [42] was simplified by eliminating the filtration step and directly analyzing the sample solution. Indeed, the comparison of the CL signals obtained by analyzing wine or instant coffee samples subjected or not to filtration showed no significant differences in the intensity of the CL signals in the test and control lines. We assumed that the sample pad was able to retain precipitated impurities avoiding their migration along the LFIA membrane.

3.6. Assay performance

To evaluate assay performance as requested for the initial in-house validation of newly developed screening methods [56] in accordance with current EU regulations [57,58] and opinions [59] we measured the detection capability ($\text{CC}\beta$) of the assay. $\text{CC}\beta$ is the smallest content of the analyte that may be detected in a sample with a given error probability (β), which for a screening assay is prescribed to be $\leq 5\%$. This means that the probability of obtaining for a sample an analyte level below regulatory limits although it is not (false compliant result) must be equal or lower than 5%.

To measure $\text{CC}\beta$, 20 blank samples of wine and 20 blank samples of instant coffee were analyzed before and after being spiked with OTA at concentrations corresponding to the maximum admissible level prescribed by the current regulatory limit (Table 2). Blank samples were previously confirmed

This item was downloaded from IRIS Università di Bologna (<https://cris.unibo.it/>)

When citing, please refer to the published version.

as compliant by verifying that their OTA contents were below the LOQ ($0.1 \mu\text{g L}^{-1}$) of the reference HPLC-FLD method.

The mean responses of blanks (B) were 0.715 and 0.700 for wine and instant coffee, respectively. The mean (M) and standard deviation (SD_M) for samples spiked at the maximum admissible levels were 0.351, 0.022 and 0.597, 0.021 for wine and instant coffee, respectively. For each matrix, the cut-off (F_m) value was calculated according to the following equation:

$$F_m = M + 1.64 SD_M$$

Since for both matrices $F_m < B$ (F_m , wine = 0.387; F_m , instant coffee = 0.631), it could be concluded that the $CC\beta$ of the assay is lower than the maximum OTA admissible levels, and therefore the assay demonstrated adequate for screening purposes [56].

The specificity of the CL-LFIA smartphone device towards other mycotoxins, specifically aflatoxins (B1, B2, G1, G2), fumonisins (B1, B2) and zearalenone, was evaluated by generating their calibration curves and calculating the concentration of mycotoxin corresponding to the midpoint of the curve (i.e., to 50% tracer bound). Then, the cross reactivity (CR) of each interfering compound was obtained as the ratio of the concentration of OTA at the midpoint of its calibration curve to the corresponding value for the compound tested. The anti-OTA antibody showed low CRs (i.e., less than 2%) with aflatoxins G1 and G2, fumonisins and zearalenone, while higher values (up to 15%) were found for aflatoxins B1 and B2 (Table 3).

3.7. Analysis of unknown samples

Finally, samples of wine (14), grape must (5) and instant coffee (6) with unknown OTA content were analyzed using the smartphone CL-LFIA device and the results were compared with those obtained with the reference HPLC-FLD method (Fig. 6). For all samples, the OTA concentration was below the regulatory limits (for three instant coffee samples the OTA content measured by HPLC-FLD was also below the LOD of the CL-LFIA assay). Recoveries of the optical biosensor ranged from 81 to 123% and variation coefficients were lower than 15%. The equation of the correlation curve is $y = 0.961x + 0.0397$ with $r^2 = 0.993$, where y and x are the OTA concentrations in $\mu\text{g L}^{-1}$ measured with the CL-LFIA assay and the HPLC-FLD method, respectively. Results demonstrated a good concordance between the two analytical approaches.

4. Conclusions

Motivated by the urgent need for user-friendly, rapid and affordable assays for on-site mycotoxins detection, we propose a portable biosensor suitable for quantifying OTA in wine and instant coffee samples. Applying smartphone-based detection to the traditional LFIA technique, an easy-to-use laboratory-independent detecting platform has been developed to be used by non-skilled personnel for real-time and on-site analysis. The CL detection allowed accurate and precise OTA quantification in the interval of concentrations of legal relevance, while one step forward was the development of a self-contained disposable fluidic cartridge with a long shelf-life (up to one year at +4 °C), to simplify the analytical procedure and reduce the consumption of samples and reagents. This biosensor can

This item was downloaded from IRIS Università di Bologna (<https://cris.unibo.it/>)

When citing, please refer to the published version.

be thus proposed for a reliable and cost-effective first-level monitoring of OTA in wines and instant coffee. This would allow a prompt identification of suspect food batches with the possibility of early tracing the origin of the contamination, hence significantly improving the current food safety control system. In the future, the possibility to employ dry reagents deposited directly onto the LFIA strip would allow to reduce the number of analysis steps and simplify the layout of the fluidic cartridge. Moreover, an ad-hoc smartphone app would guide step by step the operator in the execution of the assay and in the processing of experimental data.

Funding

This work was supported by the Italian Ministry for University and Research in the framework of “Bando 450 PRIN 2017”, project number 2017YER72K.

CRedit authorship contribution statement

Martina Zangheri: Investigation, Methodology, Writing – original draft. *Fabio Di Nardo*: Methodology, Investigation. *Donato Calabria*: Validation, Formal analysis. *Elisa Marchegiani*: Validation, Formal analysis. *Laura Anfossi*: Conceptualization, Methodology. *Massimo Guardigli*: Visualization, Writing – review & editing. *Mara Mirasoli*: Conceptualization, Writing – review & editing. *Claudio Baggiani*: Supervision. *Aldo Roda*: Supervision.

Declaration of competing interest

The authors declare that they have no known competing financial interests or personal relationships that could have appeared to influence the work reported in this paper.

References

- [1] <https://www.who.int/health-topics/foodborne-diseases> (Accessed 9 December 2020).
- [2] R. Popovic, B. Radovanov, J.W. Dunn, Food scare crisis: the effect on Serbian dairy market, *Int. Food Agribus. Manag. Rev.* 20 (2017) 113-127.
- [3] K. Yang, H. Peretz-Soroka, Y. Liu, F. Lin, Novel developments in mobile sensing based on the integration of microfluidic devices and smartphones, *Lab Chip* 16 (2016) 943-958.
- [4] A. Roda, E. Micheline, M. Zangheri, M. Di Fusco, D. Calabria, P. Simoni, Smartphone-based biosensors: a critical review and perspectives, *Trac. Trends Anal. Chem.* 79 (2016) 317-325.
- [5] G. Rateni, P. Dario, F. Cavallo, Smartphone-based food diagnostic technologies: a review, *Sensors-Basel* 17 (2017) 1453.
- [6] M.Y.C. Wu, M.Y. Hsu, S.J. Chen, D.K. Hwang, T.H. Yen, C.M. Cheng, Point-of-care detection devices for food safety monitoring: proactive disease prevention, *Trends Biotechnol.* 35 (2017) 288-300.
- [7] G.M.S. Ross, M.G.E.G. Bremer, M. Nielen, Consumer-friendly food allergen detection: moving towards smartphone-based immunoassays, *Anal. Bioanal. Chem.* 410 (2018) 5353-5371.
- [8] Y. Lu, Z. Shi, Q. Liu, Smartphone-based biosensors for portable food evaluation, *Curr. Opin. Food Sci.* 28 (2019) 74-81.

This item was downloaded from IRIS Università di Bologna (<https://cris.unibo.it/>)

When citing, please refer to the published version.

- [9] D.D. Uyeh, W. Shin, Y. Ha, T. Park, Food safety applications, in: J.-Y. Yoon (Ed.), *Smartphone Based Medical Diagnostics*, Academic Press, London, 2020, pp. 209-232.
- [10] A.F. Coskun, J. Wong, D. Khodadadi, R. Nagi, A. Tey, A. Ozcan, A personalized food allergen testing platform on a cellphone, *Lab Chip* 13 (2013) 636-640.
- [11] H. Zhu, U. Sikora, A. Ozcan, Quantum dot enabled detection of Escherichia coli using a cellphone, *Analyst* 137 (2012) 2541-2544.
- [12] P.-S. Liang, T.S. Park, J.-Y. Yoon, Rapid and reagentless detection of microbial contamination within meat utilizing a smartphone-based biosensor, *Sci. Rep.* 4 (2014) 5953.
- [13] J.A. DuVall, C.B. Juliane, N. Shafagati, D. Luzader, N. Shukla, J. Li, K. Kehn-Hall, M.M. Kendall, S.H. Feldman, J.P. Landers, Optical imaging of paramagnetic bead-DNA aggregation inhibition allows for low copy number detection of infectious pathogens, *PLoS One* 10 (2015), e0129830.
- [14] B. Jin, Y. Yang, R. He, Y.I. Park, A. Lee, D. Bai, F. Li, T.J. Lu, F. Xu, M. Lin, Lateral flow aptamer assay integrated smartphone-based portable device for simultaneous detection of multiple targets using upconversion nanoparticles, *Sensor. Actuator. B Chem.* 276 (2018) 48-56.
- [15] M.M.A. Zeinhom, Y. Wang, L. Sheng, D. Du, L. Li, M.-J. Zhu, Y. Lin, Smartphone based immunosensor coupled with nanoflower signal amplification for rapid detection of Salmonella enteritidis in milk, cheese and water, *Sensor. Actuator. B Chem.* 261 (2018) 75-82.
- [16] M.M.A. Zeinhom, Y. Wang, Y. Song, M.-J. Zhu, Y. Lin, D. Du, A portable smartphone device for rapid and sensitive detection of E. coli O157: H7 in yoghurt and egg, *Biosens. Bioelectron.* 99 (2018) 479-485.
- [17] S.K.J. Ludwig, H. Zhu, S. Phillips, A. Shiledar, S. Feng, D. Tseng, A.L. van Ginkel, M.W.F. Nielen, A. Ozcan, Cellphone-based detection platform for rbST biomarker analysis in milk extracts using a microsphere fluorescence immunoassay, *Anal. Bioanal. Chem.* 406 (2014) 6857-6866.
- [18] L. Bueno, G.N. Meloni, S.M. Reddy, T.R.L.C. Paixao, Use of plastic-based analytical device, smartphone and chemometric tools to discriminate amines, *RSC Adv.* 5 (2015) 20148-20154.
- [19] R. Monosik, V. Bezerra dos Santos, L. Angnes, A simple paper-strip colorimetric method utilizing dehydrogenase enzymes for analysis of food components, *Anal. Methods* 7 (2015) 8177-8184.
- [20] P. Masawat, H. Antony, A. Namwong, An iPhone-based digital image colorimeter for detecting tetracycline in milk, *Food Chem.* 184 (2015) 23-29.
- [21] Z. Li, Z. Li, D. Zhao, F. Wen, J. Jiang, D. Xu, Smartphone-based visualized microarray detection for multiplexed harmful substances in milk, *Biosens. Bioelectron.* 87 (2017) 874-880.
- [22] W. Xiao, C. Huang, F. Xu, J. Yan, H. Bian, Q. Fu, K. Xie, L. Wang, Y. Tang, A simple and compact smartphone-based device for the quantitative readout of colloidal gold lateral flow immunoassay strips, *Sensor. Actuator. B Chem.* 266 (2018) 63-70.
- [23] M. Eskola, G. Kos, C.T. Elliott, J. Hajslova, S. Mayar, R. Krska, Worldwide contamination of food-crops with mycotoxins: validity of the widely cited 'FAO estimate' of 25%, *Crit. Rev. Food Sci. Nutr.* 60 (2020) 2773-2789.
- [24] R.R.M. Paterson, N. Lima, How will climate change affect mycotoxins in food? *Food Res. Int.* 43 (2010) 1902-1914.
- [25] B.S. Sekhon, Nanotechnology in agri-food production: an overview, *Nanotechnol. Sci. Appl.* 7 (2014) 31-53.
- [26] P. LeDuc, M. Agaba, C.-M. Cheng, J. Gracio, A. Guzman, A. Middelberg, Beyond disease, how biomedical engineering can improve global health, *Sci. Transl. Med.* 6 (2014) 266fs48.

This item was downloaded from IRIS Università di Bologna (<https://cris.unibo.it/>)

When citing, please refer to the published version.

- [27] G.A. Evtugyn, R.V. Shamagsumova, T. Hianik, in: A.M. Grumezescu (Ed.), *Biosensors for Detection Mycotoxins and Pathogenic Bacteria in Food*, Nanobiosensors Academic Press, London, 2017, pp. 35-92.
- [28] J.L.D. Nelis, A.S. Tsagkaris, M.J. Dillon, J. Hajslova, C.T. Elliott, Smartphone-based optical assays in the food safety field, *Trac. Trends Anal. Chem.* 129 (2020) 115934.
- [29] S. Lee, G. Kim, J. Moon, Performance improvement of the one-dot lateral flow immunoassay for aflatoxin B1 by using a smartphone-based reading system, *Sensors* 13 (2013) 5109-5116.
- [30] J.M. Machado, R.R. Soares, V. Chu, J.P. Conde, Multiplexed capillary microfluidic immunoassay with smartphone data acquisition for parallel mycotoxin detection, *Biosens. Bioelectron.* 99 (2018) 40-46.
- [31] T. Sergeyeva, D. Yarynka, E. Piletska, R. Linnik, O. Zaporozhets, O. Brovko, S. Piletsky, A. El'skaya, Development of a smartphone-based biomimetic sensor for aflatoxin B1 detection using molecularly imprinted polymer membranes, *Talanta* 201 (2019) 204-210.
- [32] R.R.M. Paterson, N. Lima, Toxicology of mycotoxins, in: A. Luch (Ed.), *Molecular, Clinical and Environmental Toxicology. Experientia Supplementum*, vol. 100, Birkhauser Basel, 2010, pp. 31-63.
- [33] A. Pfohl-Leszkowicz, R.A. Manderville, Review on Ochratoxin A: an overview Fig. 6. Correlation between OTA concentrations measured in real samples using the smartphone CL-LFIA device and the reference HPLC-FLD method on toxicity and carcinogenicity in animals and humans, *Mol. Nutr. Food Res.* 51 (2007) 61-99.
- [34] European commission, Commission Regulation (EC) No 1881/2006 of 19 December 2006 setting maximum levels for certain contaminants in foodstuffs, *Off. J. Eur. Communities L364* (2006) 5-24.
- [35] Health Canada, Canadian Food and drug regulations. http://www.cfs.gov.hk/english/programme/programme_rafs/files/cfs_news_ras_23_och.pdf. (Accessed 12 September 2020).
- [36] D. Caputo, G. de Cesare, L.S. Dolci, M. Mirasoli, A. Nascetti, A. Roda, R. Scipinotti, Microfluidic chip with integrated a-Si:H photodiodes for chemiluminescence-based bioassays, *IEEE Sensor. J.* 13 (2013) 2595-2602.
- [37] M. Zangheri, L. Cevenini, L. Anfossi, C. Baggiani, P. Simoni, F. Di Nardo, A. Roda, A simple and compact smartphone accessory for quantitative chemiluminescence-based lateral flow immunoassay for salivary cortisol detection, *Biosens. Bioelectron.* 64 (2015) 63-68.
- [38] M. Zangheri, F. Di Nardo, M. Mirasoli, L. Anfossi, A. Nascetti, D. Caputo, G. De Cesare, M. Guardigli, C. Baggiani, A. Roda, Chemiluminescence lateral flow immunoassay cartridge with integrated amorphous silicon photosensors array for human serum albumin detection in urine samples, *Anal. Bioanal. Chem.* 408 (2016) 8869-8879.
- [39] A. Nascetti, M. Mirasoli, E. Marchegiani, M. Zangheri, F. Costantini, A. Porchetta, L. Iannascoli, N. Lovecchio, D. Caputo, G. de Cesare, S. Pirrotta, A. Roda, Integrated chemiluminescence-based lab-on-chip for detection of life markers in extraterrestrial environments, *Biosens. Bioelectron.* 123 (2019) 195-203.
- [40] A. Roda, F. Arduini, M. Mirasoli, M. Zangheri, L. Fabiani, N. Colozza, E. Marchegiani, P. Simoni, D. Moscone, A challenge in biosensors: is it better to measure a photon or an electron for ultrasensitive detection? *Biosens. Bioelectron.* 155 (2020) 112093.
- [41] A. Roda, S. Cavalera, F. Di Nardo, D. Calabria, S. Rosati, P. Simoni, B. Colitti, C. Baggiani, M. Roda, L. Anfossi, Dual lateral flow optical/chemiluminescence immunosensors for the rapid detection of salivary and serum IgA in patients with COVID-19 disease, *Biosens. Bioelectron.* 172 (2021) 112765.

This item was downloaded from IRIS Università di Bologna (<https://cris.unibo.it/>)

When citing, please refer to the published version.

- [42] L. Anfossi, C. Giovannoli, G. Giraudi, F. Biagioli, C. Passini, C. Baggiani, A lateral flow immunoassay for the rapid detection of ochratoxin A in wine and grape must, *J. Agric. Food Chem.* 60 (2012) 11491-11497.
- [43] G. Giraudi, V.E.V. Ferrero, L. Anfossi, C. Baggiani, C. Giovannoli, C. Tozzi, Solid-phase extraction of ochratoxin A from wine based on a binding hexapeptide prepared by combinatorial synthesis, *J. Chromatogr. A* 1175 (2007) 174-180.
- [44] A.S. Tsagkaris, J.L.D. Nelis, G.M.S. Ross, S. Jafari, J. Guercetti, K. Kopper, Y. Zhao, K. Rafferty, J.P. Salvador, D. Migliorelli, G.I.J. Salentijn, K. Campbell, M.P. Marco, C.T. Elliot, M.W.F. Nielen, J. Pulkrabova, J. Hajslova, Critical assessment of recent trends related to screening and confirmatory analytical methods for selected food contaminants and allergens, *Trac. Trends Anal. Chem.* 121 (2019) 115688.
- [45] G. Sciotto, M. Zangheri, L. Anfossi, M. Guardigli, S. Prati, M. Mirasoli, F. Di Nardo, C. Baggiani, R. Mazzeo, A. Roda, Miniaturized biosensors to preserve and monitor cultural heritage: from medical to conservation diagnosis, *Angew. Chem. Int. Ed.* 57 (2018) 7385-7389.
- [46] M. Zangheri, M. Mirasoli, M. Guardigli, F. Di Nardo, L. Anfossi, C. Baggiani, P. Simoni, M. Benassai, A. Roda, Chemiluminescence-based biosensor for monitoring astronauts' health status during space missions: results from the International Space Station, *Biosens. Bioelectron.* 129 (2019) 260-268.
- [47] S. Rattle, O. Hofmann, C.P. Price, L.J. Kricka, D. Wild, Lab-on-a-Chip, micro-and nanoscale immunoassay systems, and microarrays, in: D. Wild (Ed.), *The Immunoassay Handbook 4th Edition. Theory and Applications of Ligand Binding, ELISA and Related Techniques*, Elsevier Science, 2013, pp. 175-202.
- [48] L. Anfossi, F. Di Nardo, C. Giovannoli, C. Passini, C. Baggiani, Increased sensitivity of lateral flow immunoassay for ochratoxin A through silver enhancement, *Anal. Bioanal. Chem.* 405 (2013) 9859e9867.
- [49] H. Jiang, X. Li, Y. Xiong, K. Pei, L. Nie, Y. Xiong, Silver nanoparticle-based fluorescence-quenching lateral flow immunoassay for sensitive detection of ochratoxin A in grape juice and wine, *Toxins* 9 (2017) 83.
- [50] L. Liu, L. Xu, S. Suryoprabowo, S. Song, H. Kuang, Development of an immunochromatographic test strip for the detection of ochratoxin A in red wine, *Food Agric. Immunol.* 29 (2018) 434-444.
- [51] H.K. Oh, H.A. Joung, M. Jung, H. Lee, M.G. Kim, Rapid and simple detection of ochratoxin A using fluorescence resonance energy transfer on lateral flow immunoassay (FRET-LFI), *Toxins* 11 (2019) 292.
- [52] B.H. Liu, Z.J. Tsao, J.J. Wang, F.Y. Yu, Development of a monoclonal antibody against ochratoxin A and its application in enzyme-linked immunosorbent assay and gold nanoparticle immunochromatographic strip, *Anal. Chem.* 80 (2008) 7029-7035.
- [53] L. Wang, W. Ma, W. Chen, L. Liu, W. Ma, Y. Zhu, L. Xu, H. Kuang, C. Xu, An aptamer-based chromatographic strip assay for sensitive toxin semiquantitative detection, *Biosens. Bioelectron.* 26 (2011) 3059-3062.
- [54] L. Wang, W. Chen, W. Ma, L. Liu, W. Ma, Y. Zhao, Y. Zhu, L. Xu, H. Kuang, C. Xu, Fluorescent strip sensor for rapid determination of toxins, *Chem. Commun.* 47 (2011) 1574-1576.
- [55] S.S. Deshpande, *Enzyme Immunoassays: from Concept to Product Development*, Springer Science & Business Media, 1996.
- [56] <http://www.foodsmartphone.eu/index.html> (Accessed 9 December 2020).

This item was downloaded from IRIS Università di Bologna (<https://cris.unibo.it/>)

When citing, please refer to the published version.

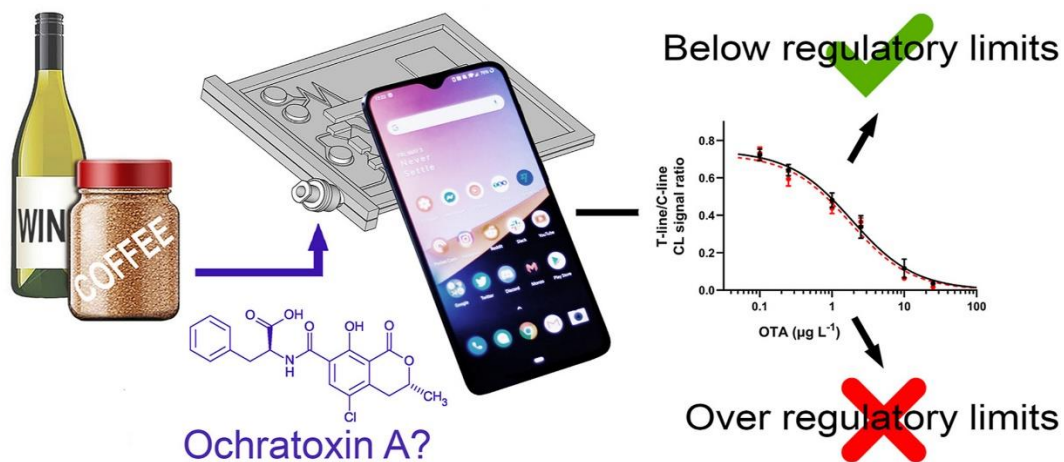
[57] Commission Decision 2002/657/EC.

[58] Commission Regulation (EU) No 519/2014 of 16 May 2014.

[59] Community Reference Laboratories Residues, Guidelines for the Validation of Screening Methods for Residues of Veterinary Medicines, 20 January 2010.

This item was downloaded from IRIS Università di Bologna (<https://cris.unibo.it/>)

When citing, please refer to the published version.



Graphical abstract

This item was downloaded from IRIS Università di Bologna (<https://cris.unibo.it/>)

When citing, please refer to the published version.

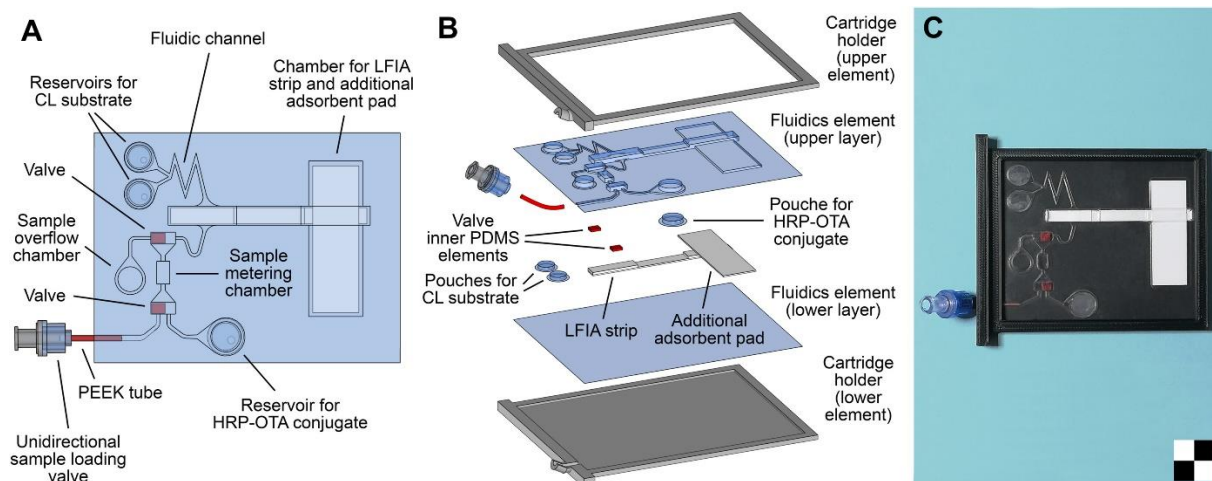


Fig. 1. Schematic drawings of the fluidic element (A), showing the different components and their fluidic connections, and of the disposable analytical cartridge (B), and photograph of the disposable analytical cartridge (C).

This item was downloaded from IRIS Università di Bologna (<https://cris.unibo.it/>)

When citing, please refer to the published version.

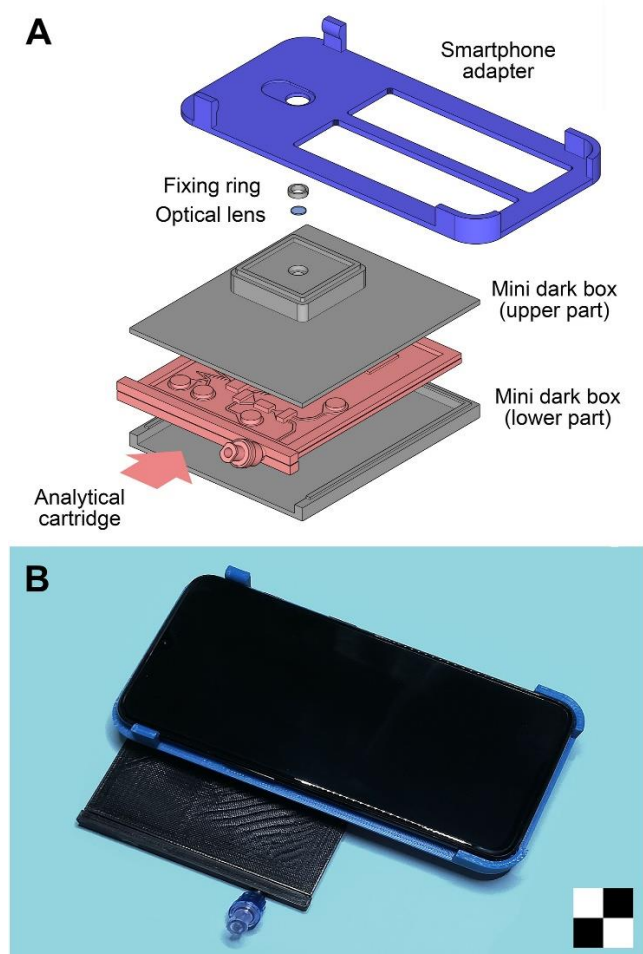


Fig. 2. Schematic drawing of the mini dark box with the smartphone adapter (A). Photograph of the LFIA-CL device with a disposable analytical cartridge and connected to the OnePlus 6 smartphone (B).

This item was downloaded from IRIS Università di Bologna (<https://cris.unibo.it/>)

When citing, please refer to the published version.

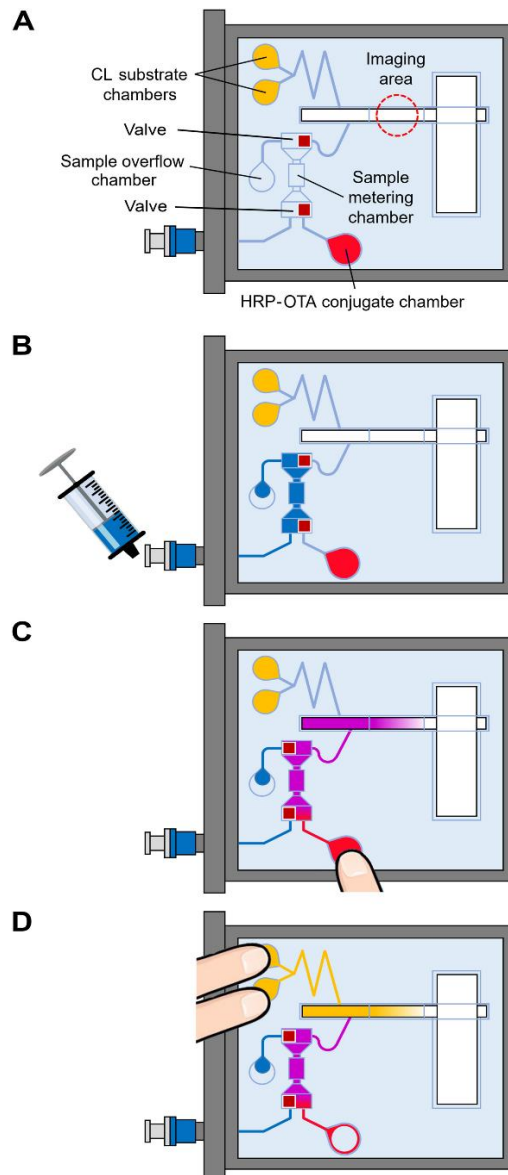


Fig. 3. Schematic representation of the analytical cartridge (A) and of the assay procedure steps: sample loading (B), transfer of the sample and the HRP-OTA conjugate solution to the LFIA strip (C), transfer of the HRP CL substrate to the LFIA strip (D).

This item was downloaded from IRIS Università di Bologna (<https://cris.unibo.it/>)

When citing, please refer to the published version.

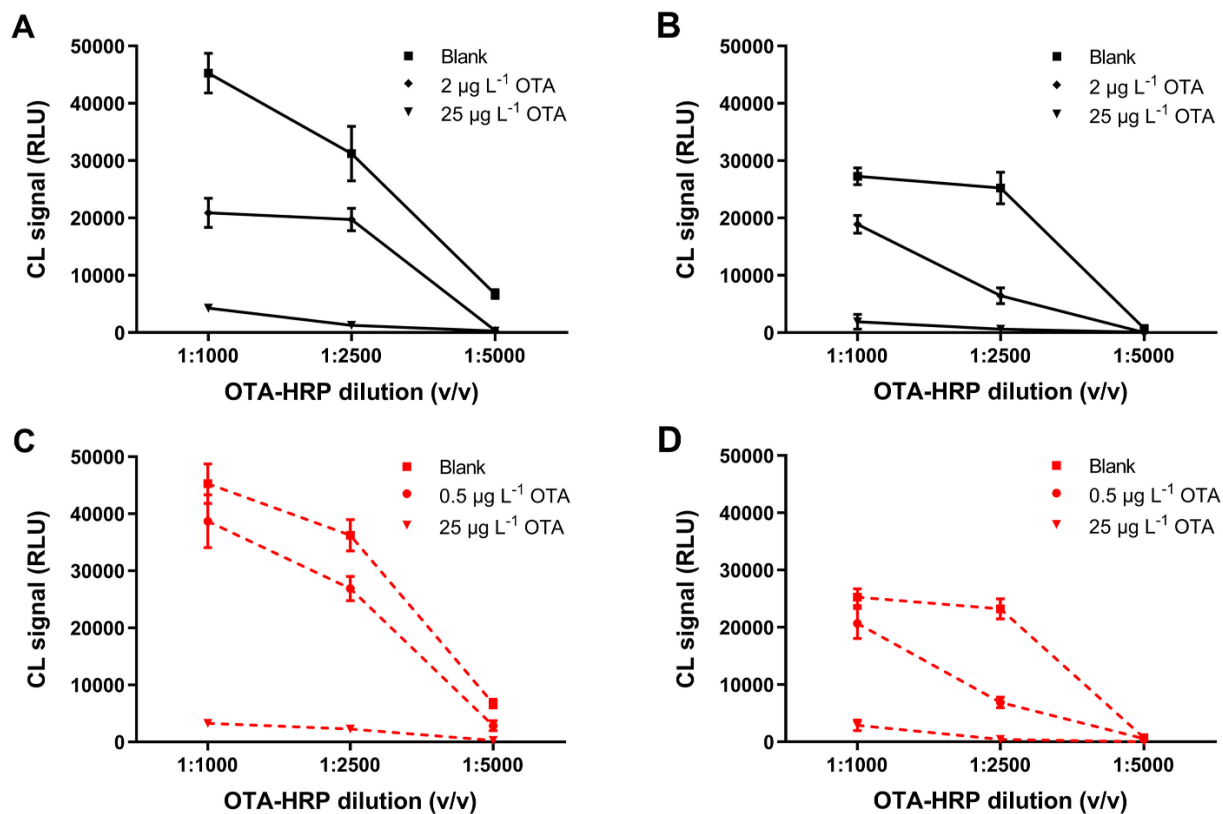


Fig. 4. Chemiluminescence signals obtained in correspondence of the T-line employing LFIA strips in which the immobilized anti-OTA antibody was dispensed at (A, C) 1:50 and (B, D) 1:100 (v/v) dilutions. Assays were performed in OTA-free wine (A, B) and instant coffee matrices (C, D), before and after spiking with OTA at the maximum admissible levels ($2 \mu\text{g L}^{-1}$ and $0.5 \mu\text{g L}^{-1}$ for wine and instant coffee matrices, respectively) and at high concentration ($25 \mu\text{g L}^{-1}$).

This item was downloaded from IRIS Università di Bologna (<https://cris.unibo.it/>)

When citing, please refer to the published version.

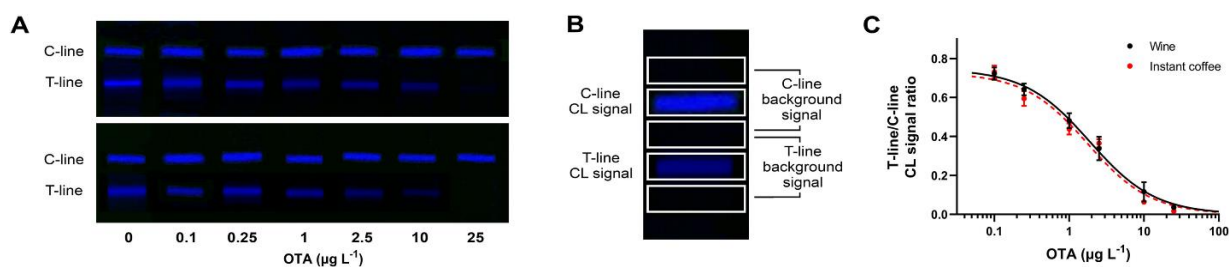


Fig. 5. (A) CL images obtained by analysing OTA-free wine and instant coffee samples spiked with known amounts of OTA. (B) Areas on the LFIA strip used for the measurement of the CL signals. (C) Representative calibration curves obtained in wine and instant coffee matrices (each standard solution was analyzed in triplicate).

This item was downloaded from IRIS Università di Bologna (<https://cris.unibo.it/>)

When citing, please refer to the published version.

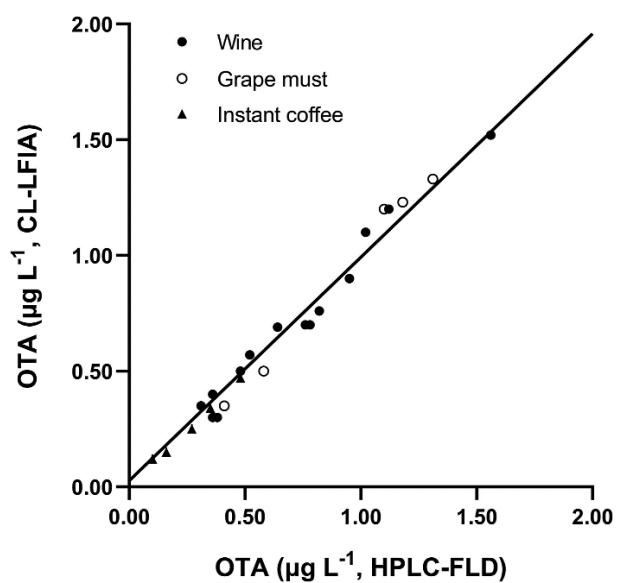


Fig. 6. Correlation between OTA concentrations measured in real samples using the smartphone CL-LFIA device and the reference HPLC-FLD method.

This item was downloaded from IRIS Università di Bologna (<https://cris.unibo.it/>)

When citing, please refer to the published version.

Table 1. Comparison of LODs of literature and commercial LFIA-based OTA assays.

Sample	Detection principle	LOD	Reference or assay trade name/producer
Wine Grape must	Colorimetry (instrumental detection)	1 $\mu\text{g L}^{-1}$	[42]
Wine Grape must	Colorimetry (instrumental detection)	0.9 $\mu\text{g L}^{-1}$	[48]
Wine Grape juice	Fluorescence (instrumental detection)	0.06 $\mu\text{g L}^{-1}$	[49]
Wine	Colorimetry (visual detection)	10 $\mu\text{g L}^{-1}$	[50]
Coffee	Fluorescence (instrumental detection)	0.88 $\mu\text{g L}^{-1}$	[51]
Coffee	Colorimetry (visual detection)	5 $\mu\text{g L}^{-1}$	[52]
Wine	Colorimetry (visual or instrumental detection)	1 $\mu\text{g L}^{-1}$ (visual detection) 0.18 $\mu\text{g L}^{-1}$ (instrumental detection)	[53]
Wine	Fluorescence (visual or instrumental detection)	5 $\mu\text{g L}^{-1}$ (visual detection) 1.9 $\mu\text{g L}^{-1}$ (instrumental detection)	[54]
Wine Grape juice	Colorimetry (instrumental detection)	1 $\mu\text{g L}^{-1}$	OCHRAQ-W Test (Charm Sciences Inc., Lawrence, MA)
Coffee	Colorimetry (instrumental detection)	1.1 $\mu\text{g L}^{-1}$	Reveal® Q + MAX for Ochratoxin (NEOGEN, Lansing, MI)
Wine	Colorimetry (instrumental detection)	0.4 $\mu\text{g L}^{-1}$	QuickTox for QuickScan Ochratoxin (EnviroLogix Inc., Portland, MA)

This item was downloaded from IRIS Università di Bologna (<https://cris.unibo.it/>)

When citing, please refer to the published version.

Table 2. T-line/C-line CL intensity ratios measured for blank wine and instant coffee samples before and after spiking with OTA at the maximum admissible levels prescribed by the current regulatory limits.

Wine			Instant coffee		
Sample no.	Before spiking T-line/C-line ratio	After spiking with 2 µg L ⁻¹ OTA T-line/C-line ratio	Sample no.	Before spiking T-line/C-line ratio	After spiking with 0.5 µg L ⁻¹ OTA ^(a) T-line/C-line ratio
1	0.746	0.349	1	0.683	0.588
2	0.727	0.320	2	0.694	0.622
3	0.712	0.372	3	0.701	0.578
4	0.719	0.387	4	0.726	0.617
5	0.708	0.320	5	0.708	0.591
6	0.684	0.359	6	0.694	0.575
7	0.701	0.336	7	0.705	0.575
8	0.712	0.350	8	0.708	0.568
9	0.719	0.348	9	0.726	0.573
10	0.691	0.375	10	0.673	0.631
11	0.746	0.363	11	0.726	0.612
12	0.658	0.336	12	0.673	0.573
13	0.723	0.327	13	0.666	0.611
14	0.746	0.381	14	0.726	0.578
15	0.727	0.391	15	0.726	0.553
16	0.684	0.360	16	0.694	0.611
17	0.746	0.348	17	0.683	0.611
18	0.746	0.324	18	0.701	0.581
19	0.712	0.342	19	0.694	0.604
20	0.701	0.334	20	0.698	0.622

^aThis concentration corresponds to 10 µg kg⁻¹ in the solid sample.

This item was downloaded from IRIS Università di Bologna (<https://cris.unibo.it/>)

When citing, please refer to the published version.

Table 3. Cross reactivity values measured for the anti-OTA antibody.

Mycotoxin	Cross reactivity
Aflatoxin B1	12%
Aflatoxin B2	15%
Aflatoxin G1	1.5%
Aflatoxin G2	1.0%
Fumonisin B1	0.9%
Fumonisin B2	0.7%
Zearalenone	1.7%

This item was downloaded from IRIS Università di Bologna (<https://cris.unibo.it/>)

When citing, please refer to the published version.